Ubiquitin Proteasome System Role in Diabetes-Induced Cardiomyopathy

Ortal Nahum-Ankonina , Efrat Kurtzwald-Josefson , Aaron Ciechanover , Maayan Waldman , Orna Schwartz Rohaker , Edith Hochhauser , Sam j Meyer , Dan Aravot , Moshe Philip , Yaron D. Barac *

Posted Date: 11 August 2023

doi: 10.20944/preprints202308.0895.v1

Keywords: UPS; T2DM; Heart

Article

Ubiquitin Proteasome System Role in Diabetes-Induced Cardiomyopathy

Ortal Nahum-Ankonina [1,2], Efrat Kurtzwald-Josefson [1], Aaron Ciechanover [3], Maayan Waldman [1], Orna Shwartz-Rohaker [1], Edith Hochhauser [1,2], Sam J. Meyer [1,2], Dan Aravot [1,2], Moshe Phillip [2,4] and Yaron D. Barac [1,2,*]

[1] The Division of Cardiovascular and Thoracic Surgery, Rabin Medical Center, Petach-Tikva, Israel
[2] Tel Aviv University, Sackler Faculty of Medicine, Tel Aviv, Israel
[3] Technion-Israel Institute of Technology, Haifa, Israel
[4] The Division of Endocrinology, Schneider Medical Center, Petach-Tikva, Israel
* Correspondence: yaronbar@clalit.org.il|

Abstract: This study investigated modifications in the ubiquitin proteasome system (UPS) in a mouse model of type 2 diabetes mellitus (T2DM) and their relationship to heart complications. *db*/*db* mice heart tissues were compared with *WT* mice tissues using RNA sequencing, qRT-PCR, and protein analysis to identify cardiac UPS modifications associated with diabetes. The findings unveiled a distinctive gene profile in the hearts of *db*/*db* mice with decreased levels of *nppb* mRNA and increased levels of *Myh7*, indicating potential cardiac dysfunction. mRNA levels of *USP18* (deubiquitinating enzyme), *psmb8*, and *psmb9* (proteasome β-subunits) were downregulated in *db*/*db* mice while mRNA levels of RNF167 (E3 ligase) were increased. Corresponding LMP2 and LMP7 proteins were downregulated in *db*/*db* mice, and RNF167 was elevated in *Adult* diabetic mice. Reduced expression of LMP2 and LMP7, along with increased RNF167 expression, may contribute to future cardiac deterioration commonly observed in diabetes. This study enhances our understanding of UPS imbalances in the hearts of diabetic mice and raises questions about the interplay between the UPS and other cellular processes, such as autophagy. Further exploration in this area could provide valuable insights into the mechanisms underlying diabetic heart complications and potential therapeutic targets.

Keywords: UPS; T2DM; Heart

1. Introduction

Type 2 diabetes mellitus (T2DM) is a disease commonly attributed to pancreatic insufficiency, inadequate insulin secretion, or increased insulin resistance, and accounts for the vast of all diabetes cases worldwide [1]. The number of people with T2DM has dramatically increased over the past decade and is expected to reach 592 million by 2035 [2]. This growing prevalence combined with an increasingly young onset of the disease have established T2DM as a global health concern and garnered significant attention in the literature over the past decade [3]. T2DM patients are shown to carry a higher risk of numerous complications including cardiovascular diseases [4], as T2DM compromises the cardiac tissue, causing cell damage, impaired calcium homeostasis, mitochondrial dysfunction, changes in muscle fibers, oxidative stress, and inflammation [5,6]. All of these cellular changes have been shown to cause heart failure and ischemic heart disease [7].

The UPS plays a central role in the regulation of many cellular processes in the body, such as cell cycle [8], cellular signaling [9] and programmed cell death [10]; Consequently, deviations in UPS activity underlie the pathogenesis of various diseases [11]. Specifically, UPS oversees cellular protein quality control by driving degradation of misfolded and/or damaged proteins via poly-ubiquitination of target proteins. There are three types of enzymes that promote this process: ubiquitin-activating enzymes (E1), ubiquitin-conjugating enzymes (E2), and ubiquitin-ligating

Preprints (www.preprints.org) | NOT PEER-REVIEWED | Posted: 11 August 2023 doi:10.20944/preprints202308.0895.v1

enzymes (E3). Initially, E1 binds a ubiquitin molecule forming an ATP-dependent thioester linkage. The ubiquitin relocates to an E2 enzyme, which either transfers the ubiquitin to E3 directly or binds to E3 as an adaptor protein. Together E2 and E3 attach ubiquitin to a lysine residue on the target protein [12,13], (Figure 1A). E3 ubiquitin ligases are known to define the substrate- and tissue-specificity of the UPS and are considered to play a significant role in maintaining protein quality control. This role is especially vital in maintaining cardiac tissue function due to its poor regenerative capacity [14].

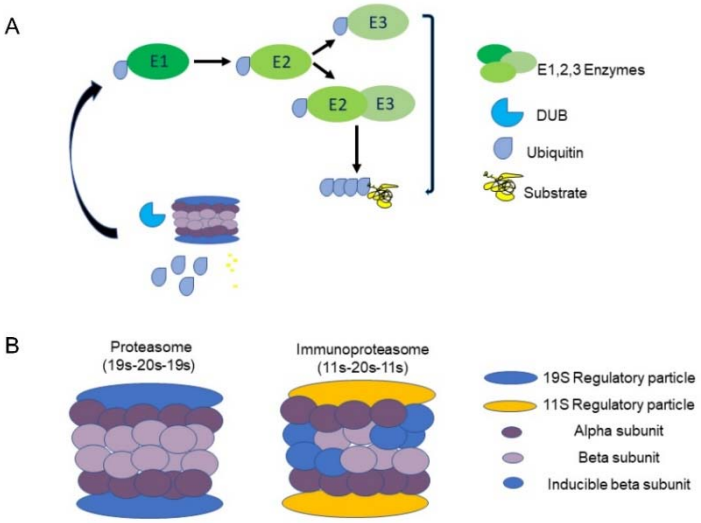

Figure 1. The ubiquitin proteasome system: **(A)** Three types of enzymes promote degradation; ubiquitin-activating enzymes (E1), ubiquitin-conjugating enzymes (E2), and ubiquitin-ligating enzymes (E3). Initially, E1 binds a ubiquitin molecule forming an ATP-dependent thioester linkage. The ubiquitin relocates to an E2 enzyme, which either transfers the ubiquitin to E3 directly or binds to E3 as an adaptor protein. Together E2 and E3 attach ubiquitin to a lysine residue on the target protein. Deubiquitinating enzymes (DUBs) sort ubiquitinated proteins remove and recycle ubiquitin. (**B**) A constitutive proteasome 19S-20S-19S (left) and immunoproteasome 11S-20S-11S (right).

After a cellular protein is tagged with a chain of at least four ubiquitin molecules, it is recognized and degraded by the 26S proteasome complex [13]. The barrel-shaped proteasome contains a 20S core particle and a 19S regulatory particle (RP) that binds 20S bilaterally, forming a 19S-20S-19S (30S) complex. 20S is responsible for the complex's ATP-dependent catalytic activity and is composed of two external α rings and two internal β rings [15], with each ring comprising seven distinct subunits (α 1-7, β 1-7). In some cases, an 11S (PA28) RP, replaces the 19S, forming either the 11S-20S-11S or the 19S-20S-11S hybrid (Figure 1B). These forms enable ubiquitin-independent degradation [16]. Some 11S-20S-11S complexes contain replacements of the 1, 2 and 5 β subunits with inducible counterparts, such as β1i (LMP2, encoded by *PSMB9*), β2i (MECL-1, encoded by *PSMB10*) and β5i (LMP7 encoded by *PSMB8*), respectively [17]. This transformation is triggered by IFN-γ and is referred to as the 'immunoproteasome'.

Considering the cardiac changes that occur in the diabetic heart, we hypothesized that UPS malfunction might play a central role in early diabetes, leading to cardiac pathology. These changes may set the stage for future diabetes induced heart failure and deterioration. Our aim was to identify such early events that might provide a better understanding of the mechanisms leading to diabetes-induced heart failure and inform future treatment of these patients.

2. Results

db/*db* mice were used to explore the effects of the UPS in diabetic induced cardiomyopathy [18-20]. Blood glucose levels, body weight, heart weight, and heart/body weight ratio were measured in

Preprints (www.preprints.org) | NOT PEER-REVIEWED | Posted: 11 August 2023 doi:10.20944/preprints202308.0895.v1

Young and *Adult db/db* and *WT* mice (Figure 2). Glucose levels were higher in *Adult db/db* mice compared to *Adult WT* mice, ($p<0.0001$), (Figure 2A). Furthermore, the body weight of both *Young* and *Adult db/db* mice was significantly higher than that of age-matched *WT* mice (Figure 2B). Heart/body weight ratio was significantly lower in *db/db* as compared to *WT* mice, in both *Adult* and *Young* groups (Figure 2D).

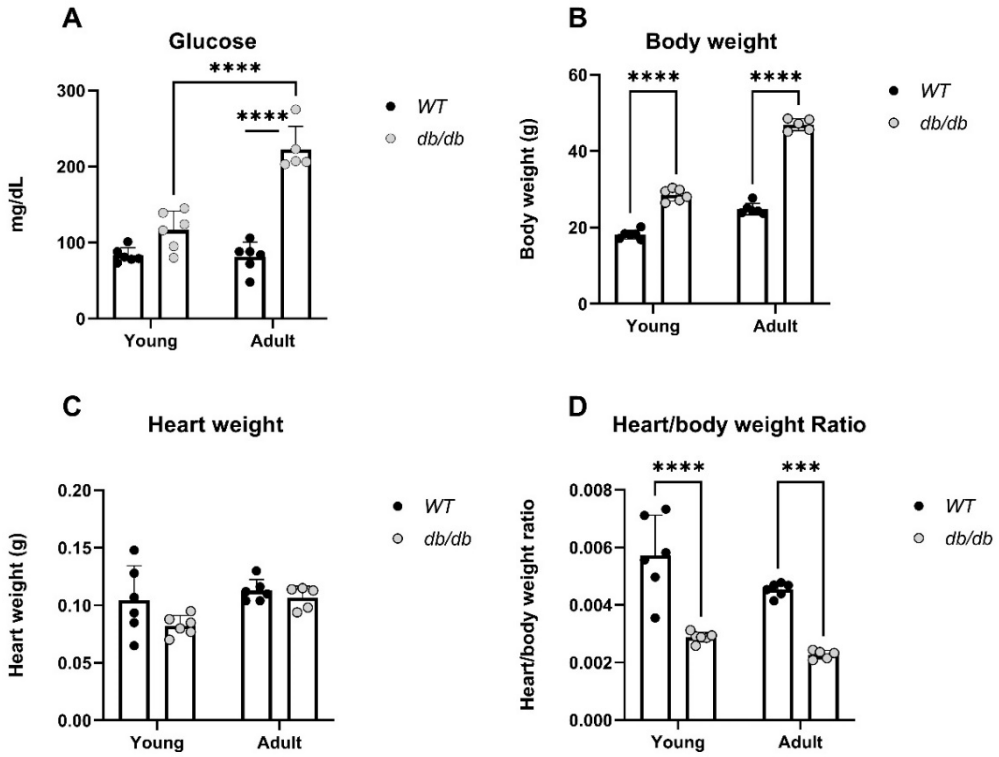

Figure 2. Physiological differences obtained by glucose, body weight and heart weight measurements of *Young* and *Adult db/db* and *WT* mice. Y: 4-8-week-old. A: 11-18-week-old. Glucose: WT_y: n=6, db_y: n=6, WT_a: n=6, db_a: n=5, (**A**). Body weight: WT_y: n=6, db_y: n=6, WT_a: n=6, db_a: n=5, (**B**). Heart weight: WT_y: n=6, db_y: n=6, WT_a: n=6, db_a: n=5, (C). Heart/body weight .

Echocardiographic (ECHO) recordings of 16-week-old *db/db* and *WT* mice were taken (Table 1). The results identified a smaller left ventricular end systolic diameter (LVESD) in *db/db* mice, compared to *WT* ($p<0.05$) and a tendency to a higher end diastolic dimension. No other echocardiographic parameters, including the fractional shortening (FS), were significantly different between the groups.

Table 1. Echocardiography: Interventricular septum (IVS), left ventricular posterior wall (LVPW), left ventricular end dimension diastole/systole (LVEDD/LVESD respectively), fractional shortening (FS%). T-test * $p < 0.05$.

Preprints (www.preprints.org) | NOT PEER-REVIEWED | Posted: 11 August 2023 doi:10.20944/preprints202308.0895.v1

	WT n=7	*db/db* n=11
IVS (mm)	0.8±0.1	0.9±0.1
LVPW (mm)	0.9±0.1	0.9±0.1
LVEDD (mm)	3.6±0.7	3.9±0.2
LVESD (mm)	2.9±0.2	2.6±0.3*
FS (%)	33±14	34±7

Proteasome activity is different in *db/db* mice. Proteins extracted from the hearts of *Young* and *Adult db/db* mice and their age-matched *WT* mice were subjected to a proteasome activity assay. *Young db/db* mice exhibited reduced 20S proteasome activity compared with *Young WT* mice (Figure 3). Furthermore, while the *WT* mice exhibited progressively less activity with age, the *db/db* mice exhibited an opposite trend, with an increase in 20S activity (Figure 3).

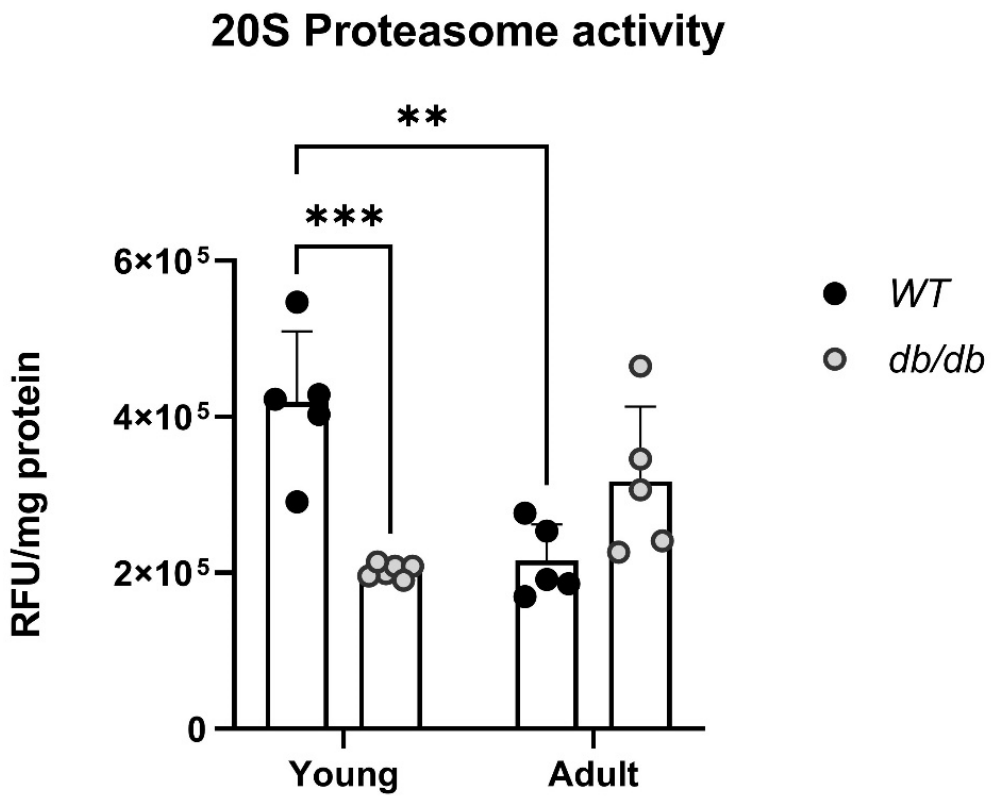

Figure 3. Abnormal 20S proteasome activity in diabetic mice. *Young*: 6-week-old (y), *Adult*: 12-week-old (a) WT_y: n=5, db_y: n=6, WT_a: n=5 db_a: n=5, Two-way ANOVA ** $p < 0.01$, *** $p < 0.001$.

2.1. RNA sequencing emphasizes the differences between db/db and WT mice

RNA sequencing was performed on RNA samples extracted from cardiac tissues and compared with that of *WT* mice. A principal component analysis (PCA) plot representing the experiment variance was based on the gradual change in expression of approximately 5000 genes. PCA determined four homogenous groups as expected (Figure 4A). The variation in gene expression observed between *Young* and *Adult db/db* mice points to a greater change in gene expression when

Preprints (www.preprints.org) | NOT PEER-REVIEWED | Posted: 11 August 2023 doi:10.20944/preprints202308.0895.v1

the *db/db* mice transition from the pre-diabetic to the diabetic state. Differential expression (DE) analysis found vast differences in gene expression (> 500 genes) between *Young db/db* and *Young WT* mice and between *Adult db/db* and *Adult WT* mice. The exact number of modified genes, including the directional change in their expression (up- or downregulation), is summarized in Figure 4.

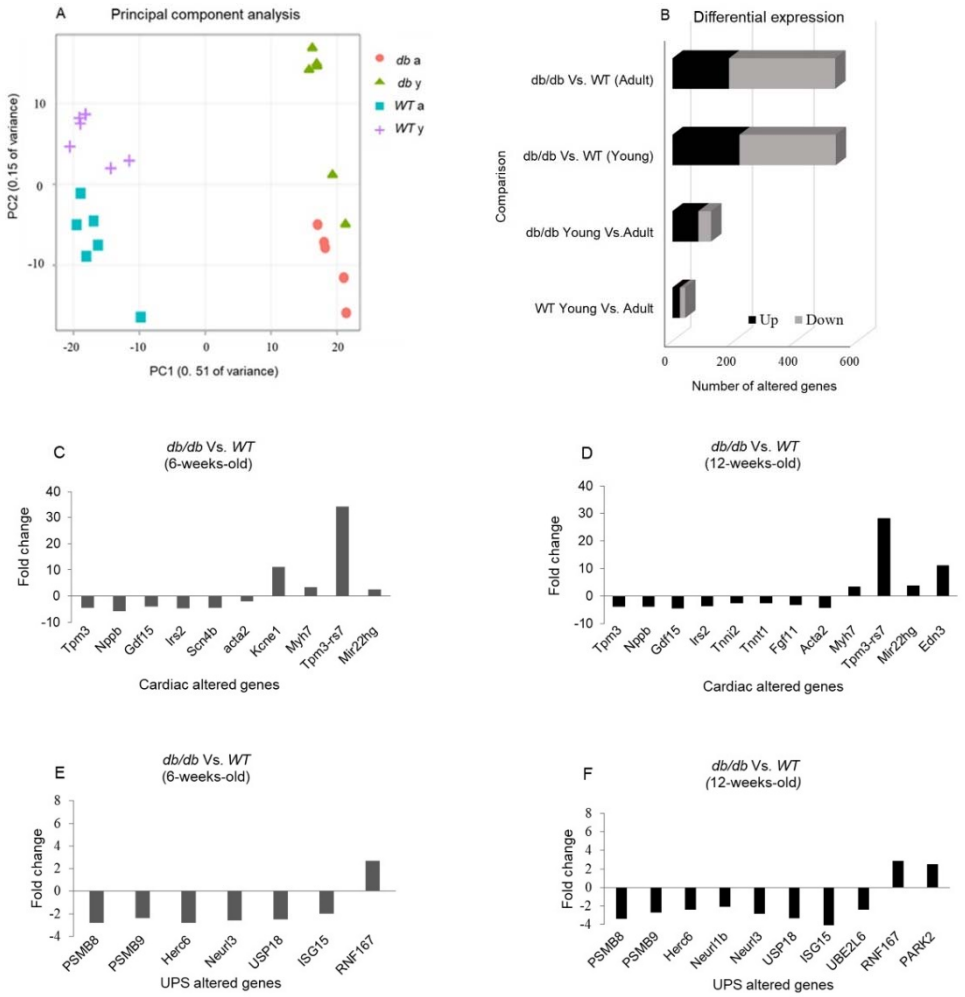

Figure 4. RNA sequencing of cardiac samples detected changes in over 500 genes. A principal component analysis (PCA) was performed to present the sample differences according to gene expression levels. Threshold for significance was set at p adjusted ≤≤ 0.05, Max counts per gene ≥≥ 30, |Fold Change| ≥≥ 2 (**A**). Differential expression (DE) comparisons found major gene expression differences between age-matched *db/db* and WT mice groups (**B**). DE of cardiomyopathy (**C**-**D**)- and UPS-related genes (**E**-**F**) detected by RNA sequencing in young (4-8-week-old) and adult (11-18-week-old) *db/db* vs. WT mice.

2.2. Cardiomyopathy-and UPS related genes are differently expressed in db/db compared with WT mice

mRNA levels of cardiomyopathy-and UPS-related genes were evaluated. Cardiomyopathy-related genes such as B-type natriuretic peptide (*nppb*), [21], encoding the BNP protein, an indicator of heart failure, and myosin heavy chain 7 (*Myh7*) [22], encoding the beta (slow) heavy chain subunit of cardiac myosin, were both altered in *db/db* mice compared with *WT* mice. While *nppb* was downregulated in diabetic mice regardless of age, differences were only significant in the comparison of *Adult* mice ($p<0.01$) (Figure 5A). In contrast, *Myh7* mRNA level was increased in *Adult db/db* mice ($p=0.05$) (Figure 5B). mRNA levels of tropomyosin alpha-3 (*Tpm3*), encoding the protein which stabilizes actin, were reduced with age in *WT* mice but increased with age in *db/db* mice (Figure 5C).

Preprints (www.preprints.org) | NOT PEER-REVIEWED | Posted: 11 August 2023 doi:10.20944/preprints202308.0895.v1

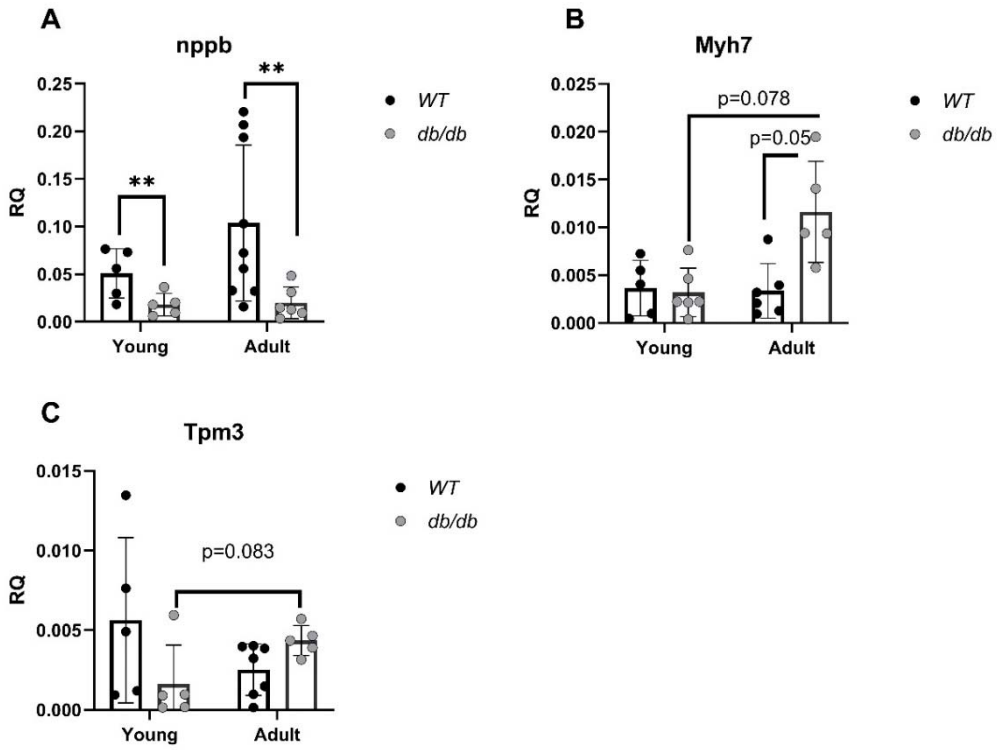

Figure 5. Cardiomyopathy-related gene alterations in diabetic mice, detected by qRT-PCR. *RNF167* (n=5) (**A**), *USP18* (n=5), (**B**), *Isg15* (n=WT_y: n=5, db_y: n=5, WT_a: n=5, db_a: n=6) (**C**), *Ube2l6* (n=WT_y: n=5, db_y: n=5, WT_a: n=5, db_a: n=6) (**D**), *nppb* (n=WT_y: n=5, db_y: n=5, WT_a: n=9, db_a: n=7) (**E**). *Myh7* (n=WT_y: n=5, db_y: n=5, WT_a: n=6, db_a: n=5) (**F**). *Tpm3*: (n=WT_y: n=5, db_y: n=5, WT_a: n=7, db_a: n=5) (**G**). Results are normalized to *GAPDH*. *P< 0.05, ** P< 0.01 using a Two-way ANOVA with interaction.

Gene expression of immunoproteasome components including the 11S α-unit and the three inducible β subunits, β5i, β1i, and β2i (encoded by: *Psme1, Psmb8, Psmb9* and *Psmb10*, respectively) were significantly reduced in *Adult db/db* mice compared with *Adult WT* mice and regardless of age (Figure 6A-6D).

Preprints (www.preprints.org) | NOT PEER-REVIEWED | Posted: 11 August 2023 doi:10.20944/preprints202308.0895.v1

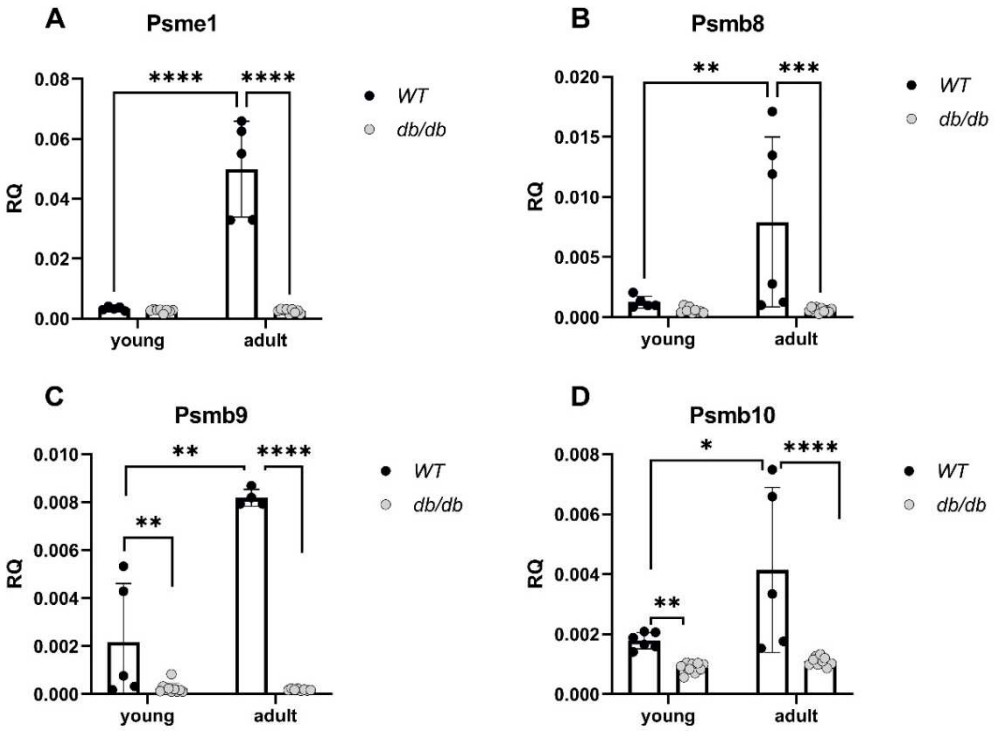

Figure 6. Reduced expression of genes encoding for immunoproteasome components in diabetic mice. mRNA levels of proteasome component genes were compared between *db/db* and *WT* mice. *Psme1*: WT_y: n=5, db_y: n=5, WT_a: n=8, db_a: n=9, (**A**), *Psmb8*: WT_y: n=5, db_y: n=6, WT_a: n=8, db_a: n=9, (**B**). *Psmb9*: WT_y: n=5, db_y: n=4, WT_a: n=10, db_a: n=8, (**C**). *Psmb10*: WT_y: n=6, db_y: n=5, WT_a: n=9, db_a: n=9, (**D**). Results are normalized to GAPDH. Two-way ANOVA. * p< 0.05, ** p< 0.01, *** p< 0.001, **** p< 0.0001.

In parallel, mRNA levels of *RNF167*, a gene encoding an E3 ubiquitin ligase, were elevated in *Adult* diabetic mice compared with *Adult WT* mice (P<0.05), (Figure 7A). Expression of *USP18*, a deubiquitinating enzyme (DUB), was significantly lower in diabetic mice compared with *WT* mice (p<0.05), (Figure 7B). *Isg15*, encoding the ubiquitin-like protein- USP18 substrate, was significantly downregulated in diabetic mice compared with *WT*, regardless of age (p<0.01), (Figure 7C). *Trim54* and *Trim63*, both encoding E3 ligases, were significantly altered. While *Trim54* was significantly upregulated in *Adult* diabetic mice compared to *Young* diabetic mice (p<0.01), (Figure 7E), *Trim63* was downregulated in diabetic mice, regardless of age, (p<0.001), (Figure 7F).

Preprints (www.preprints.org) | NOT PEER-REVIEWED | Posted: 11 August 2023 doi:10.20944/preprints202308.0895.v1

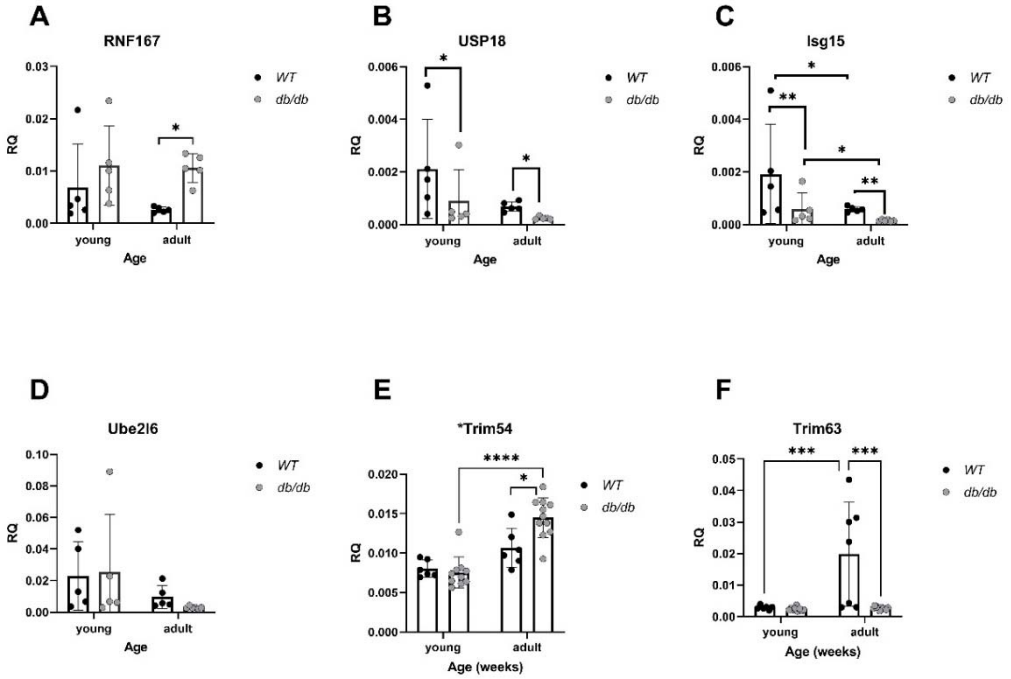

Figure 7. Alterations in UPS-related gene expression in diabetic mice: mRNA levels of UPS genes were compared between *db/db* and *WT* mice. *RNF167*: All groups: n=5, (**A**). *USP18*: All groups: n=5, (**B**). *Isg15:* WT_y: n=5, db_y: n=5, WT_a: n=5, db_a: n=6, (**C**). *Ube2l6*: WT_y: n=5, db_y: n=5, WT_a: n=5, db_a: n=6, (**D**), *Trim54 (Murf3)*: WT_y: n=6, db_y: n=6, WT_a: n=10, db_a: n=11, (**E**). *Trim63 (Murf1)*: WT_y: n=6, db_y: n=7, WT_a: n=9, db_a: n=10, (F). Results are normalized to GAPDH. Two-way ANOVA * $p< 0.05$, ** $p< 0.01$, *** $p< 0.001$, **** $p< 0.0001$.

2.3. UPS-related protein expression in db/db mice

A trend of increasing RNF167 protein levels was detected in *Young db/db* mice, while levels were significantly increased in *Adult db/db* mice (Figure 8A). LMP2 and LMP7 were both downregulated in *Adult db/db* mice (Figure 8B-C).

Preprints (www.preprints.org) | NOT PEER-REVIEWED | Posted: 11 August 2023 doi:10.20944/preprints202308.0895.v1

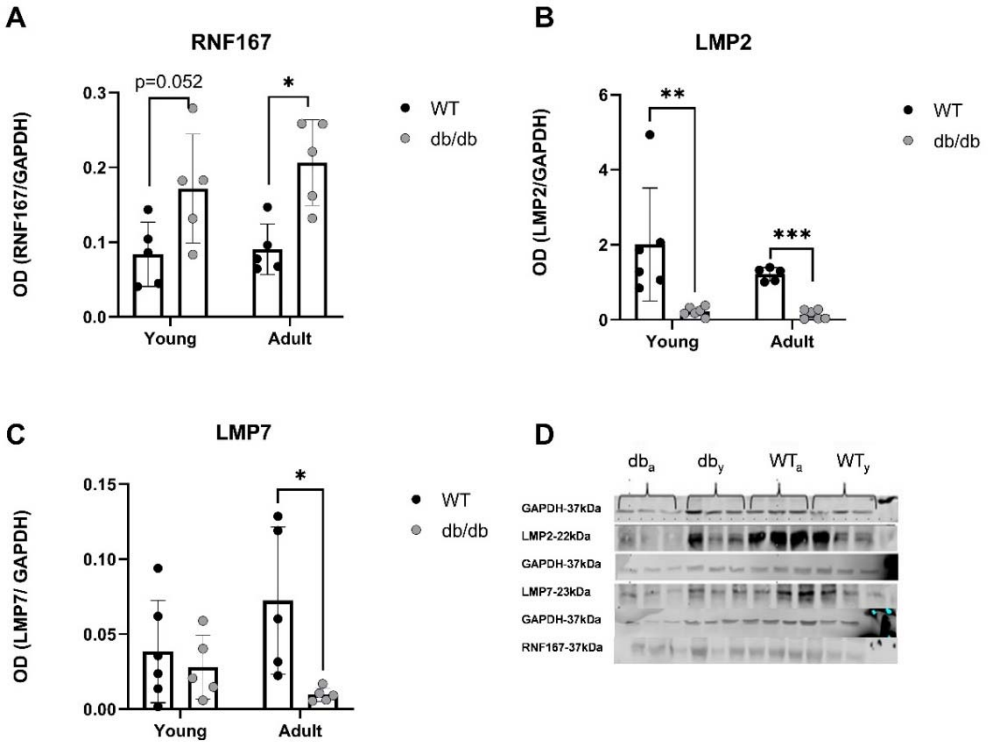

Figure 8. UPS-related proteins are expressed differently in the heart of *db*/*db* mice compared with WT. Proteins expression was evaluated using western blot analysis. RNF176 (n=5) (**A**), LMP2 (n=5-6) (**B**) and LMP7 (n=5-6) (**C**), P<0.05) (**D**), *p< 0.05, **P<0.01. Multiple Mann-Whitney.

3. Discussion

The study investigated changes in UPS-related gene expression in the heart tissue of *db*/*db* mice at different stages of diabetes progression. The analysis revealed that genetic changes in UPS components were already detectable in *Young*, pre-diabetic mice, indicating an early alteration in UPS activity.

Young db/*db* mice are considered pre-diabetic, and transition to fully diabetic at approximately 12 weeks of age [18]. Blood glucose levels in pre-diabetic *db*/*db* mice were slightly higher than in age-matched *WT* mice, with a significant value at the *Adult* group (Figure 2A). Heart/body weight ratio significantly declined with age in *WT*. This decline is likely due to the greater increase in body and heart weight of *db*/*db* mice, while leaving the heart/body weight ratio nearly unchanged (Figure 2D). Differences of UPS expression in diabetic myocardial tissue, were already noted with *Young db*/*db* exhibiting reduced 20S proteasome activity compared to *WT* (Figure 3). The 20S reduced activity aligns with reports by Predmore and colleagues, demonstrating reduced proteasomal activity in failing hearts [23]. The 20S proteasome can remain free or bind to either 19S or 11S regulator units [24] while 11S can improve 20S ability to specifically locate oxidized proteins. Based on our RNA-seq analysis, genes encoding the 19S particles were not different among the groups, however genes encoding the immunoproteasome and several cardiac genes expressed significant differences-(Figure 4E-4F). *nppb*- a circulatory hormone and a heart failure biomarker was reduced in diabetic mice (Figure 5A) in line with findings reported by Zhang et al, who found that *nppb* synthesis is reduced following onset of systemic insulin resistance in mice [21]. *Myh7*, was upregulated in *db*/*db* mice (Figure 5B), suggesting a change in cardiac muscle composition, with possible implications on contractility and functionality. Overexpression of *PSME1*, a gene encoding the PA28α unit of 11S, was found to have a positive effect in diabetic and hyperglycemic rat hearts [25, 26]. The current study detected a reduction in *PSME1* mRNA levels in *db*/*db* mice (Figure 6A), while in *WT* mice, *PSME1* mRNA levels increased with age. These findings underscore the importance of *PSME1* in healthy cardiac tissue.

 doi:10.20944/preprints202308.0895.v1

We observed that the mRNA levels of immunoproteasome β subunits, specifically upregulated under stress conditions [27], increased with age in *WT* mice but not in *db*/*db* mice (Figure 6B-D). This suggests a reduced cellular response to oxidative stress in the diabetic heart, which can further impair protein homeostasis.

E3 ubiquitin ligases hold central role in the progression of cardiovascular pathologies [27] e.g. cardiac hypertrophy, apoptosis inhibition [28, 29], regulation of cardiac reactive oxygen species (ROS) [30]. We found upregulation of *RNF167* mRNA levels in *db*/*db* mice (Figure 7A), and significant increase in expression of its protein in *Adult db*/*db* mice (Figure 8A). RNF167 upregulation may simultaneously relate to several mechanisms including autophagy and proteasome degradation, both of which impact cellular protein homeostasis. RNF167 has been implicated in the regulation of lysosomal exocytosis [31], of the α-amino-3-hydroxy-5-methyl-4-isoxazolepropionic acid glutamate receptor (AMPAR). RNF167 along with neural precursor cell-expressed developmentally downregulated gene 4-1 (Nedd4-1) were shown to facilitate ubiquitination of AMPAR in mammalian neurons, [32] and thereby regulate cell-cell communication [33]. However, no difference in Nedd4-1 RNA levels was detected between *db*/*db* and *WT* mice, further highlighting the specificity of RNF167 upregulation in diabetic mice.

We detected a few changes in mitophagy-related genes in diabetic mice. For example, BCL2/adenovirus-interacting protein 3 (*BNIP3*), a mitophagy marker known to be upregulated by the c-Jun N-terminal protein kinase (JNK) pathway in ER-stressed cells and to affect contractility [34], was downregulated compared with *WT* mice. *PARK2* (Parkin), which enhances mitophagy by ubiquitinating mitochondria [35], was upregulated in *Adult* diabetic mice. No changes in any other autophagy genes, such as *ATGs*, *LC3*, or *PINK1* were detected. The limited autophagy-related gene changes detected by RNA-seq in diabetic mice further support our hypothesis of a unique UPS compensatory mechanism underlying diabetic cardiomyopathy.

DUBs sort ubiquitinated proteins to authorize their entry into the proteasome thereby remove and recycle ubiquitin [36]. Reduced expression of USP18, a DUB involved in regulating inflammation, was observed in diabetic mice (Figure 7B), suggesting an impaired UPS regulation in the early prediabetes stages.

Reductions in LMP2 (β1i) and LMP7 (β5i) protein levels were also detected, indicating suboptimal functioning of the UPS in diabetic hearts. LMP7, is necessary for balanced protein homeostasis in a healthy aging heart [37]. Here, we detected a reduction of both LMP2 and LMP7 protein levels in *Adult* diabetic mice, suggesting a general immune susceptibility of the diabetic heart. While upregulation of immunoproteasome genes and proteins was expected, these findings proved incongruous with this prediction as the ratio of proteasome/immunoproteasome activity decreased in the heart with age.

Optimal functioning of cardiac UPS components including proteasome, immunoproteasome and E3 ligases, is essential to healthy cardiac function. The presented findings confirm a genetic UPS imbalance in *db*/*db* cardiac tissue. This improves our understanding of changes to protein homeostasis in the heart that either precede or accompany diabetes development and include a wide range of UPS players. These findings also raise questions regarding the crosstalk between UPS and other cellular processes such as autophagy, mitophagy, and lysosome trafficking in the diabetic heart. Future research should focus on characterizing the network of UPS players and their respective roles in healthy heart function. Such data may assist in diagnosing UPS imbalances and may identify biomarkers of early-stage cardiac stress prior to a diabetic diagnosis.

4. Materials and Methods

To test this hypothesis, we monitored UPS component expression in the hearts of *db*/*db Young* (pre-diabetic) and *Adult* (diabetic) mice, a T2DM model.

Animal model for T2DM: The animal experiments were approved by the Tel Aviv University Institutional Animal Care and Use Committee.Two strains of mice were used: BLKS/J -Leprdb/-Leprdb/OlaHsd (*db*/*db*) mice (a model for type 2 diabetes) and C57BLKs/6JOlaHsd (*WT*) mice (wild-

Preprints (www.preprints.org) | NOT PEER-REVIEWED | Posted: 11 August 2023 doi:10.20944/preprints202308.0895.v1

type control). Mice were acclimated for two weeks in a pathogen-free facility and provided regular rodent chow and water ad libitum.

Animal study design: Mice were divided into two age groups: *Young* (4-8 weeks old) and *Adult* (11-18 weeks old).

Glucose measurements: Blood glucose levels were measured in mice after a 12-hour fast using a Glucometer. Mice were weighed and anesthetized with 2% isoflurane inhalation and blood samples were collected from the tail vein for glucose measurement.

Echocardiographic recordings: Mice were anesthetized with 2% isoflurane inhalation. Echocardiography was performed using a Vevo 2100 Imaging System with a 30-MHz linear transducer. Two-dimensional (2D) guided M-mode echocardiography was used to assess heart function. Left-ventricular end-diastolic dimensions (LVEDD) and left-ventricular end-systolic chamber dimensions (LVESD) were measured. Left-ventricular fractional shortening (FS) was calculated as a measure of cardiac function.

RNA extraction from heart tissue: RNA was extracted from heart tissue using the RNeasy Fibrous Tissue Mini Kit. The extracted RNA was quantified using a NANODROP and evaluated for RNA integrity using an RNA integrity number (RIN).

Genomics: RNA sequencing was performed at The Crown Genomics Institute of the Nancy and Stephen Grand Israel National Center for Personalized Medicine. Libraries were prepared using the G-INCPM mRNAseq protocol. Sequencing was performed using the Illumina HiSeq machine. Bioinformatics analysis was conducted to identify differentially expressed (DE) genes and determine relevant biological functions and pathways.

Quantitative real-time polymerase chain reaction (qPCR): cDNA was prepared from RNA samples using the TaqMan High-capacity cDNA Reverse Transcription (RT) kit. qPCR was performed using the Stepone Real-Time PCR cycler. Specific primers were used for amplification, and gene expression levels were quantified using the 2^(-ΔCT) method.

Table 2. A list of primers used for qRT-PCR.

Gene primers	Catalog number	Company
GAPDH	Mm99999915_g1	Applied Biosystems, ThermoFisher scientific, CA, USA
PSME1	Mm00650858_g1	Applied Biosystems, ThermoFisher scientific, CA, USA
PSMB8	Mm01278980_g1	Applied Biosystems, ThermoFisher scientific, CA, USA
PSMB9	Mm00479004_g1	Applied Biosystems, ThermoFisher scientific, CA, USA
PSMB10	Mm00479052_g1	Applied Biosystems, ThermoFisher scientific, CA, USA
USP18	Mm01188805_m1	Applied Biosystems, ThermoFisher scientific, CA, USA
ISG15	Mm01705338_s1	Applied Biosystems, ThermoFisher scientific, CA, USA
RNF167	Mm00550965_m1	Applied Biosystems, ThermoFisher scientific, CA, USA
UBE2l6	Mm00498295_m1	Applied Biosystems, ThermoFisher scientific, CA, USA
Myh7	Mm00600555_m1	Applied Biosystems, ThermoFisher scientific, CA, USA
Nppb	Mm01255770_g1	Applied Biosystems, ThermoFisher scientific, CA, USA
Tpm3	Mm04336671_g1	Applied Biosystems, ThermoFisher scientific, CA, USA

Protein analysis and 20S Proteasome activity: Protein extraction from heart tissue and cells was performed using appropriate buffers. Western blot analysis was conducted to detect protein expression using specific antibodies. 20S proteasome activity was measured using a fluorescence-based assay.

Preprints (www.preprints.org) | NOT PEER-REVIEWED | Posted: 11 August 2023 doi:10.20944/preprints202308.0895.v1

Table 3. List of antibodies used for western blotting.

Primary antibodies	Cat number	Company
GAPDH (1:1000)	sc-36502	Santa Cruz Biotechnology, Texas, USA
RNF167 (1:100)	ab185099	Abcam, Cambridge, UK
Lmp2 (1:100)	ab3328	Abcam, Cambridge, UK
Lmp7 (1:100)	ab3329	Abcam, Cambridge, UK
Secondary antibodies	**Cat number**	**Company**
Goat anti-rabbit IgG, IRDye®800RD (1:10000)	925-32213	LI-COR Corporate, Nebraska, USA
Donkey anti-mouse IgG, IRDye®680RD (1:10000)	925-98072	LI-COR Corporate, Nebraska, USA

Statistical analysis: Data are presented as mean ± standard deviation. Differences between experimental groups were analyzed using two-way analysis of variance (ANOVA) followed by a Tukey test or the Mann–Whitney non-parametric test. A p-value of < 0.05 was considered statistically significant.

Conflicts of Interest: The authors declare no conflict of interest

References

1. Deshpande, A.D., M. Harris-Hayes, and M. Schootman, *Epidemiology of diabetes and diabetes-related complications.* Phys Ther, 2008. **88**(11): p. 1254-64.
2. Kenny, H.C. and E.D. Abel, *Heart Failure in Type 2 Diabetes Mellitus.* Circ Res, 2019. **124**(1): p. 121-141.
3. Tiderencel, K.A., D.A. Hutcheon, and J. Ziegler, *Probiotics for the treatment of type 2 diabetes: A review of randomized controlled trials.* Diabetes Metab Res Rev, 2020. **36**(1): p. e3213.
4. Berg, D.D., et al., *Heart Failure Risk Stratification and Efficacy of Sodium-Glucose Cotransporter-2 Inhibitors in Patients With Type 2 Diabetes Mellitus.* Circulation, 2019. **140**(19): p. 1569-1577.
5. Boudina, S. and E.D. Abel, *Diabetic cardiomyopathy, causes and effects.* Rev Endocr Metab Disord, 2010. **11**(1): p. 31-9.
6. Pappachan, J.M., et al., *Diabetic cardiomyopathy: Pathophysiology, diagnostic evaluation and management.* World J Diabetes, 2013. **4**(5): p. 177-89.
7. Kawata, T., et al., *Coronary microvascular function is independently associated with left ventricular filling pressure in patients with type 2 diabetes mellitus.* Cardiovasc Diabetol, 2015. **14**: p. 98.
8. Castro, A., et al., *The anaphase-promoting complex: a key factor in the regulation of cell cycle.* Oncogene, 2005. **24**(3): p. 314-25.
9. Ciechanover, A., A. Orian, and A.L. Schwartz, *Ubiquitin-mediated proteolysis: biological regulation via destruction.* Bioessays, 2000. **22**(5): p. 442-51.
10. Jesenberger, V. and S. Jentsch, *Deadly encounter: ubiquitin meets apoptosis.* Nat Rev Mol Cell Biol, 2002. **3**(2): p. 112-21.
11. Ciechanover, A., *Proteolysis: from the lysosome to ubiquitin and the proteasome.* Nat Rev Mol Cell Biol, 2005. **6**(1): p. 79-87.
12. Glickman, M.H. and A. Ciechanover, *The ubiquitin-proteasome proteolytic pathway: destruction for the sake of construction.* Physiol Rev, 2002. **82**(2): p. 373-428.
13. Wenzel, D.M., K.E. Stoll, and R.E. Klevit, *E2s: structurally economical and functionally replete.* Biochem J, 2011. **433**(1): p. 31-42.
14. Parry, T.L. and M.S. Willis, *Cardiac ubiquitin ligases: Their role in cardiac metabolism, autophagy, cardioprotection and therapeutic potential.* Biochim Biophys Acta, 2016. **1862**(12): p. 2259-2269.
15. Wang, S., et al., *Ablation of Immunoproteasome beta5i Subunit Suppresses Hypertensive Retinopathy by Blocking ATRAP Degradation in Mice.* Mol Ther, 2020. **28**(1): p. 279-292.
16. Benaroudj, N., et al., *The unfolding of substrates and ubiquitin-independent protein degradation by proteasomes.* Biochimie, 2001. **83**(3-4): p. 311-8.
17. Bitzer, A., et al., *Immunoproteasome subunit deficiency has no influence on the canonical pathway of NF-kappaB activation.* Mol Immunol, 2017. **83**: p. 147-153.
18. Ostler, J.E., et al., *Effects of insulin resistance on skeletal muscle growth and exercise capacity in type 2 diabetic mouse models.* Am J Physiol Endocrinol Metab, 2014. **306**(6): p. E592-605.

19. Kloss, A., et al., *Multiple cardiac proteasome subtypes differ in their susceptibility to proteasome inhibitors.* Cardiovasc Res, 2010. **85**(2): p. 367-75.
20. Greer, J.J., D.P. Ware, and D.J. Lefer, *Myocardial infarction and heart failure in the db/db diabetic mouse.* Am J Physiol Heart Circ Physiol, 2006. **290**(1): p. H146-53.
21. Zhang, H., et al., *Regulation of B-type natriuretic peptide synthesis by insulin in obesity in male mice.* Exp Physiol, 2016. **101**(1): p. 113-23.
22. Montag, J., et al., *Intrinsic MYH7 expression regulation contributes to tissue level allelic imbalance in hypertrophic cardiomyopathy.* J Muscle Res Cell Motil, 2017. **38**(3-4): p. 291-302.
23. Predmore, J.M., et al., *Ubiquitin proteasome dysfunction in human hypertrophic and dilated cardiomyopathies.* Circulation, 2010. **121**(8): p. 997-1004.
24. Lee, H.S., et al., *Lipotoxicity dysregulates the immunoproteasome in podocytes and kidneys in type 2 diabetes.* Am J Physiol Renal Physiol, 2021. **320**(4): p. F548-F558.
25. Powell, S.R., et al., *Upregulation of myocardial 11S-activated proteasome in experimental hyperglycemia.* J Mol Cell Cardiol, 2008. **44**(3): p. 618-21.
26. Powell, S.R., et al., *The ubiquitin-proteasome system and cardiovascular disease.* Prog Mol Biol Transl Sci, 2012. **109**: p. 295-346.
27. Shukla, S.K. and K. Rafiq, *Proteasome biology and therapeutics in cardiac diseases.* Transl Res, 2019. **205**: p. 64-76.
28. Peris-Moreno, D., D. Taillandier, and C. Polge, *MuRF1/TRIM63, Master Regulator of Muscle Mass.* Int J Mol Sci, 2020. **21**(18).
29. Portbury, A.L., et al., *Back to your heart: ubiquitin proteasome system-regulated signal transduction.* J Mol Cell Cardiol, 2012. **52**(3): p. 526-37.
30. Mattox, T.A., et al., *MuRF1 activity is present in cardiac mitochondria and regulates reactive oxygen species production in vivo.* J Bioenerg Biomembr, 2014. **46**(3): p. 173-87.
31. Nair, S.V., et al., *Naturally occurring and tumor-associated variants of RNF167 promote lysosomal exocytosis and plasma membrane resealing.* J Cell Sci, 2020. **133**(11).
32. Widagdo, J., et al., *Regulation of AMPA Receptor Trafficking by Protein Ubiquitination.* Front Mol Neurosci, 2017. **10**: p. 347.
33. Barac, Y.D., et al., *The ubiquitin-proteasome system: A potential therapeutic target for heart failure.* J Heart Lung Transplant, 2017. **36**(7): p. 708-714.
34. Bozi, L.H.M., et al., *Endoplasmic reticulum stress impairs cardiomyocyte contractility through JNK-dependent upregulation of BNIP3.* Int J Cardiol, 2018. **272**: p. 194-201.
35. Gao, F., et al., *The mitochondrial protein BNIP3L is the substrate of PARK2 and mediates mitophagy in PINK1/PARK2 pathway.* Hum Mol Genet, 2015. **24**(9): p. 2528-38.
36. Ying, X., et al., *Novel Protective Role for Ubiquitin-Specific Protease 18 in Pathological Cardiac Remodeling.* Hypertension, 2016. **68**(5): p. 1160-1170.
37. Kasacka, I., et al., *Ageing-related changes in the levels of beta-catenin, CacyBP/SIP, galectin-3 and immunoproteasome subunit LMP7 in the heart of men.* PLoS One, 2020. **15**(3): p. e0229462.